Identification of the General Anesthesia Induced Loss of Consciousness by Cross Fuzzy Entropy-Based Brain Network

Fali Li, Yuqin Li, Hui Zheng, Lin Jiang, Dongrui Gao, Cunbo Li, Yueheng Peng, Zehong Cao, Yangsong Zhang, Dezhong Yao, *Senior Member, IEEE*, Tao Xu, Ti-Fei Yuan, and Peng Xu

***Abstract*— Although the spatiotemporal complexity and network connectivity are clarified to be disrupted during the general anesthesia (GA) induced unconsciousness, it remains to be difficult to exactly monitor the fluctuation of consciousness clinically. In this study, to track the loss of consciousness (LOC) induced by GA, we first developed the multi-channel cross fuzzy entropy method to construct the time-varying networks, whose temporal fluctuations were then explored and quantitatively evaluated. Thereafter, an algorithm was further proposed to detect the time onset at which patients lost their consciousness. The results clarified during the resting state, relatively stable fuzzy fluctuations in multi-channel network architectures and properties were found; by contrast, during the LOC period, the disrupted frontal-occipital connectivity occurred at the early stage, while at the later stage, the inner-frontal connectivity was identified. When specifically exploring the early LOC stage, the uphill of the clustering coefficients and the downhill of the characteristic path length were found, which might help resolve the propofol-induced consciousness fluctuation in patients. Moreover, the developed detection algorithm was validated to have great capacity in exactly capturing the time point (in seconds) at which patients lost consciousness. The findings demonstrated that the time-varying cross-fuzzy networks help decode the GA and are of great significance for developing anesthesia depth monitoring technology clinically.**

***Index Terms*— General anesthesia, loss of consciousness, cross fuzzy entropy, time-varying networks.**

Manuscript received June 14, 2021; revised September 13, 2021; accepted October 24, 2021. Date of publication October 27, 2021; date of current version November 9, 2021. This work was supported in part by the National Natural Science Foundation of China under Grant 61961160705, Grant 62103085, Grant U19A2082, and Grant 61901077; in part by the Science and Technology Development Fund, Macau, under Grant 0045/2019/AFJ; in part by the Project of Science and Technology Department of Sichuan Province under Grant 2021YFSY0040, Grant 2018JZ0073, and Grant 2020ZYD013; in part by the Australian Research Council-Discovery Early Career Researcher Award (ARC DECRA) Fellowship under Grant DE220100265; and in part by the Key Research and Development Program of Guangdong Province, China, under Grant 2018B030339001. *(Fali Li, Yuqin Li, and Hui Zheng contributed equally to this work.) (Corresponding authors: Tao Xu; Ti-Fei Yuan; Peng Xu.)*

This work involved human subjects or animals in its research. Approval of all ethical and experimental procedures and protocols was granted by the Ethics Committee of the Shanghai Sixth People's Hospital.

Fali Li, Yuqin Li, Lin Jiang, Cunbo Li, Yueheng Peng, Dezhong Yao, and Peng Xu are with the MOE Key Laboratory for Neuroinformation, The Clinical Hospital of Chengdu Brain Science Institute, and the Center for Information in Medicine, School of life Science and Technology, University of Electronic Science and Technology of China, Chengdu 611731, China (e-mail: xupeng@uestc.edu.cn).

Hui Zheng is with the Shanghai Key Laboratory of Psychotic Disorders, Shanghai Mental Health Center, Shanghai Jiao Tong University School of Medicine, Shanghai 200030, China.

Dongrui Gao is with the School of Computer Science, Chengdu University of Information Technology, Chengdu 610225, China.

Zehong Cao is with the STEM, University of South Australia, Mawson Lakes Campus, Adelaide, SA 5095, Australia.

Yangsong Zhang is with the School of Computer Science and Technology, Southwest University of Science and Technology, Mianyang 621010, China.

Tao Xu is with the Department of Anesthesiology, Affiliated Shanghai Sixth People's Hospital, Shanghai Jiao Tong University, Shanghai 200233, China, and also with the Department of Anesthesiology, Affiliated Tongzhou People's Hospital, Nantong University, Nantong 226300, China (e-mail: balor@sjtu.edu.cn).

Ti-Fei Yuan is with the Shanghai Key Laboratory of Psychotic Disorders, Shanghai Mental Health Center, Shanghai Jiao Tong University School of Medicine, Shanghai 200030, China, also with the Co-Innovation Center of Neuroregeneration, Nantong University, Nantong 226001, China, and also with the Translational Research Institute of Brain and Brain-Like Intelligence, Shanghai Fourth People's Hospital Affiliated to Tongji University School of Medicine, Shanghai 200030, China (e-mail: ytf0707@126.com).

Digital Object Identifier 10.1109/TNSRE.2021.3123696

I. Introduction

GENERAL anesthesia (GA), a drug-induced state, comprises unconsciousness, amnesia, analgesia, and akinesia, but stays stable of the autonomic nervous system [1], [2]. If the GA is not achieved or maintained clinically, accidental intraoperative awareness occurs, which affects up to 1% of the global patients [3]. Intraoperative awareness may cause mental injury severely and then result in post-traumatic emergency disorder syndrome [4], [5]. Therefore, accurately monitoring the patients' consciousness state across the GA duration is crucial for successful clinical surgery. In clinical, the anesthesiologists usually request patients to behaviorally respond to a verbal or physical stimulus and then rate the quality of responses on a 0 - 5 numerical scale [6], [7], to testify if the patients have lost their consciousness, which seems to be subjective and temporally rough (resolution of minutes).

The electroencephalogram (EEG) that measures the scalp electrophysiological signals generated by the postsynaptic currents has been long used as a feasible technique to track consciousness states under GA [8], [9]–[11], as well as clinically monitoring the depth of the GA [12]. For example, the EEG spectral pattern is found to dynamically fluctuate along with the depth of anesthesia, and related alpha energy forward shift has thus been proved to be a potential biomarker for indexing

the propofol-induced LOC [2], [13]. Furthermore, in clinical, based on the single-channel EEG time series, related techniques have been developed, such as the BIS (Aspect Medical Systems, Newton, MA) [14] and M-entropy (GE Healthcare, Helsinki, Finland) [15] to monitor the patients' consciousness, which is derived from linear theories. As far as we know, the EEG is a non-stationary array signal and exhibits non-linear or chaotic characteristics, those GA indicators derived from linear EEG parameters may fail to measure the anesthesia depth accurately, as well as tracking the fluctuation of the consciousness during GA [16]. In fact, the human brain works as a nonlinear complex network that is composed of multi-channel interactions, related fluctuations in the network interactions have been widely found to contribute to effective information processing [17], [18], as well as facilitating the identification of different conditions [19]–[21]. Therefore focusing merely on local activity cannot reliably assess the fluctuations of related brain states, as well.

As clarified in previous studies, long-distance information exchanging, especially top-down connectivity, may serve as a crucial criterion to evaluate brain consciousness [22], [23]. If unconsciousness occurs, the breakdown within related network architectures is usually identified [24], [25], and compared to being awake, the connectivity induced by the propofol during the loss of consciousness (LOC) period also reduces. Moreover, related network architectures also shift during surgery and GA dynamically [26], and during the anesthetic maintenance phase specifically, connectivity shifts among neurophysiologic states, along with distinct oscillatory and spatial characteristics [27]. Considering the disrupted connectivity [28], [29] and reduced spatiotemporal complexity [30], [31] have been clarified to be correlated with the anesthetic unconsciousness, we thus wonder if these parameters could be the potential markers to monitor LOC and then quantitatively identify the time onset at which patients lose their consciousness in seconds?

In fact, exploring the brain state fluctuation based on the multi-sensor networks will not only deepen our understanding of consciousness fluctuation during GA but also helps monitor the LOC. Recently, when constructing related brain networks, traditional coherency and spectral estimation have been widely used [32], these approaches help characterize stationary signals and could capture the underlying multi-channel linear relations. Given the EEG is non-linear and non-stationary, traditional linear approaches thus fail in capturing the brain fluctuations accurately. On the contrary, methods based on nonlinear dynamics are believed to be helpful [16], especially entropies that are skilled in measuring the non-linear complexity of EEG signals [33]. Herein, to exactly capture the fluctuations in the nonlinear multi-channel interactions, related cross-entropies were thus considered, among which, the cross fuzzy entropy (C-FuzzyEn) [34], [35] was first considered. Compared to other cross entropies, C-FuzzyEn has the great potential in effectively avoiding undesirable boundary effects and thus guarantees related metrics to vary smoothly and continuously with similarity tolerance; in the meantime, fewer parameter definitions, better relative consistency, and less dependence on EEG data length [35], [36] also facilitate the application of C-FuzzyEn in multiple studies. Therefore, in our present study, C-FuzzyEn was accordingly considered and used in exploring the time-varying network fluctuations, as well as quantitatively monitoring the transition of patients' consciousness state.

In this study, our goal was to quantitatively measure the temporal fluctuations in time-varying brain networks during the propofol-induced GA, which would further greatly contribute to the detection of the time onset at which patients lost their consciousness. Herein, we assumed the long-range functional connectivity would be disrupted during the LOC period. To achieve an accurate assessment of the LOC, we first developed a multi-channel network method to construct the corresponding time-varying C-FuzzyEn networks, as well as exploring related network architecture fluctuations during GA; thereafter, based on related time-varying network properties, an algorithm was proposed and further used to detect the time onset at which the consciousness transited to unconsciousness in patients.

II. Materials and Methods

A. Participants

This study was approved by the Ethics Committee of the Shanghai Sixth People's Hospital. Thirty patients (age of 50.7 $\pm$ 12.6 years old) who required GA clinically for surgery were recruited in this study. Before experiments, all subjects provided written informed consent and signed their names on it, and they were also required to avoid eating for at least 8 h. All patients underwent induction of GA with propofol and inhaled sevoflurane during surgery, and the scale was maintained at 2-3%. Apart from participating in the standard pre-anesthesia assessments, all patients were also tested for normal hearing and urine toxicology to ensure that they had not taken drugs that might interact adversely with propofol or confound the EEG or behaviors. During the GA, patients inhaled a mixture of 80% air and oxygen with an oxygen content of 80% and a flow rate of 2L/min; meanwhile, their heart rate, oxygen saturation, respiration and expired carbon dioxide, and blood pressure were also simultaneously monitored.

B. EEG Data Acquisition

The 128-channel EEG datasets consisting of before-GA Resting (4 mins) and LOC (3 - 4 mins) periods were collected by using an EEG Amplifier (EGI Inc., Eugene, Oregon, USA). During data recording, the online bandpass filtering was set within [0.01, 100] Hz, the online sampling rate was set as 500 Hz, and Cz served as the reference electrode. For all electrodes, the impedance was kept consistently below 5 KΩ throughout the experiment. In particular, after collecting the Resting data, patients were transferred to the operating room and were ready to start the operation. When performing the general anesthesia, two experienced and independent anesthesiologists were recruited, in detail, the anesthesiologists administered 5ug sufentanil intravenously and then began intravenous propofol 3.5 to 4.5mg/kg according to body weight, to achieve patients' general anesthesia. Once all of

these patients were injected with propofol to induce GA, their LOC data were simultaneously recorded, and they then lost consciousness gradually and entered the anesthetic maintenance state subsequently. Herein when evaluating patients' LOC, both anesthesiologists were further required to use the same method, which was the commonly used protocol to clinically evaluate patients' unconsciousness under general anesthesia. Herein, the patient would be considered to be unconscious only after they had no spontaneous movement, no response to any stimulus, no eyelash reflex, and no response to verbal commands.

C. EEG Preprocessing

The raw EEG datasets were first exported into MATLAB (v2014a; MathWorks, Inc., USA). Both Resting and LOC data were preprocessed in compliance with the standard procedures depicted as follows. Considering the nearby electrodes acquire similar contributions from related cortical sources, they would then capture a similar activity. In this study, to reduce the effects of volume conduction on the time-varying networks, following the protocols applied in previous studies [37], [38], the sparsely distributed 19 channels over the scalp (i.e., Fp1, Fp2, F3, F4, Fz, C3, C4, P3, P4, Pz, O1, O2, Oz, F7, F8, T7, T8, P7, and P8) were selected and then re-referenced to a neutral reference of Reference Electrode Standardization Technique (REST) [39], [40]. Herein, the following analyses were further conducted mainly within the alpha band due to its characteristic connectivity directly reflecting various states of consciousness induced by anesthesia [10], [41], and accordingly, the referenced data was offline band-pass filtered within a frequency range of [8, 13] Hz. Meanwhile, considering the brain fluctuation from consciousness to unconsciousness usually occurs within a relatively short duration of [30, 60] s after being generally anesthetized [1], following a duration suggested in the previous study [29], when dividing the band-pass filtered into multiple EEG segments, a 10-s-length duration was then used. Concretely, to achieve the time-varying EEG estimation (i.e., time-varying single-channel fuzzy entropies and multi-channel C-FuzzyEn networks) during the propofol-induced GA, a 10-s-length sliding window approach with the overlapping of 90% between two adjacency segments was adopted, which could provide a 1-s-length temporal resolution. And these divided EEG segments would be further used in any following analysis.

D. Fluctuation of Consciousness State Identified by Single- and Multi-Channel Analyses

Considering the exploration of the brain fluctuation during the GA could effectively deepen our knowledge of the LOC, as well as facilitating the detection of anesthetic consciousness fluctuation in patients. Herein, based on the preprocessed EEG datasets, the single-channel fuzzy entropy (FuzzyEn) and multi-channel cross fuzzy entropy analyses were performed during both Resting and LOC periods.

E. Single-Channel Fluctuation Based on Fuzzy Entropy

Based on the single-channel time series, FuzzyEn was first applied in the artifact-free EEG signals, and the corresponding single-channel time-varying fuzzy entropy was accordingly acquired. Concretely, for each 10-s-length EEG segment, the corresponding fuzzy entropy was first calculated; thereafter, the fuzzy entropies across all 10-s-length segments formed the corresponding time-varying fuzzy entropy and then quantitatively measured the fuzzy fluctuation of patients' consciousness state during the GA.

FuzzyEn is insensitive to external disturbance (e.g., noise) but is sensitive to the fluctuation of information [42]. Thus, FuzzyEn has the great potential of effectively evaluating the fluctuation of the concerned time series, especially for the short series that are contaminated by unexpected noise [43]. Assuming there are N points in each 10-s-length single-channel segment X, its series can be termed as X_i ($1 \le i \le N$), which is formed as follows;

$$X_i^m = \{u(i), u(i+1), \ldots, u(i+m-1)\} - \bar{u}(i), \quad i = 1, \ldots, N-m+1 \tag{1}$$

where X_i^{m} comprises m consecutive u values (i.e., fluctuating magnitude) at i-th time point, which is generalized by removing the baseline $\bar{u}(i) = \frac{1}{m}\sum_{l=0}^{m-1} u(i+l)$.

Then, based on r, calculating the similarity index, D_{ij}^m, between two adjacency vectors, X_i^{m} and X_j^{m},

$$D_{ij}^m(n, r) = \mu_s(Td_{ij}^m, r) \tag{2}$$

where Td_{ij}^m denotes the maximum absolute difference of the scalar components between X_i^{m} and X_j^{m}.

For each vector X_i^{m} ($i = 1, 2, \ldots, N\text{-}m+1$), by averaging all D_{ij}^m, with its neighboring vectors X_j^{m} ($i = 1, 2, \ldots, N\text{-}m+1$, $j \ne i$), we could get φ_s^m and φ_s^{m+1},

$$\varphi_s^m(r) = \frac{1}{N-m}\sum_{i=1}^{N-m}\left(\frac{1}{N-m}\sum_{j=1, j\ne i}^{N-m} D_{ij}^m\right) \tag{3}$$

$$\varphi_s^{m+1}(r) = \frac{1}{N-m}\sum_{i=1}^{N-m}\left(\frac{1}{N-m}\sum_{j=1, j\ne i}^{N-m} D_{ij}^{m+1}\right) \tag{4}$$

And we then define the $FuzzEn(m, r)$ of the time series X_i ($1 \le i \le N$) as follow;

$$FuzzEn(m, r) = \lim_{N\to\infty}\left[\ln\varphi^m(r) - \ln\varphi^{m+1}(r)\right] \tag{5}$$

which can be estimated by the statistic,

$$FuzzEn(m, r, N) = \ln\varphi^m(r) - \ln\varphi^{m+1}(r) \tag{6}$$

where m and r denote the length of the compared window and the width of fuzzy similarity boundary, respectively, and N denotes the time series length needed to be analyzed. As proved, a larger m could guarantee a more detailed information reconstruction but an overlarge m may lead to the loss of related information, and as suggested, we then set m as 2 [44]. For r, small r may bring the noise, but the overlarge r might lose information [45], in this study, we thus set r as 0.2.

F. Multi-Channel Network Fluctuation Based on C-FuzzyEn

Given the GA has widely been interpreted as a network disruption [25], investigating the anesthetic consciousness fluctuation based on the multi-channel networks will be more helpful for monitoring the GA clinically. Herein, apart from concentrating on the single-channel EEG signal, based on the multi-channel 10-s-length EEG segments, we also developed a multi-channel C-FuzzyEn method to construct the time-varying brain networks during the propofol-induced GA. Herein, the corresponding analytical protocols were depicted in Fig. 1 and further described below.

When constructing the corresponding time-varying networks, the C-FuzzyEn approach was first applied in the EEG signals of any pairwise channels, X_i $(1 \le i \le N)$ and Y_j $(1 \le j \le N)$. Herein, apart from the single-channel EEG signal, X_i $(1 \le i \le N)$, the time series of another EEG channel was represented by Y_j $(1 \le j \le N)$, which was formed as follow:

$$Y_j^m = \{v(j), v(j+1), \ldots, v(j+m-1)\} - \bar{v}(j), \quad j = 1, \ldots, N-m+1 \tag{7}$$

where Y_j^m comprises m consecutive v values commencing with the j-th point, and its baseline, $\bar{v}$, was defined as follow,

$$\bar{v}(j) = \frac{1}{m}\sum_{l=0}^{m-1} v(j+l) \tag{8}$$

The distance, Nd_{ij}^m, between X_i^m and Y_j^m was then defined as the maximum absolute difference of their corresponding scalar components:

$$Nd_{ij}^m = \max k\, f(0, m-1)\, |u(i+k) - \bar{u}(i) - (v(j+k) - \bar{v}(j))| \tag{9}$$

Given n and r, the corresponding similarity index, ND_{ij}^m, between X_i^m and Y_j^m can be acquired by using a fuzzy function, $\mu_N(d_{ij}^m, n, r)$, and calculated as,

$$ND_{ij}^m(n, r) = \mu_N(Nd_{ij}^m, n, r) \tag{10}$$

where $\mu_N(d_{ij}^m, n, r)$ is the exponential function and defined as,

$$\mu_N\left(Nd_{ij}^m, n, r\right) = \exp\left(-\left(Nd_{ij}^m\right)^n / r\right) \tag{11}$$

Then for C-FuzzyEn, φ_N^m and φ_N^{m+1} are defined as:

$$\varphi_N^m(n, r) = \frac{1}{N-m}\sum_{i=1}^{N-m}\left(\frac{1}{N-m}\sum_{j=1}^{N-m} ND_{ij}^m\right) \tag{12}$$

$$\varphi_N^{m+1}(n, r) = \frac{1}{N-m}\sum_{i=1}^{N-m}\left(\frac{1}{N-m}\sum_{j=1}^{N-m} ND_{ij}^{m+1}\right) \tag{13}$$

Theoretically, we define the parameter, $C - FuzzyEn_{XY}(m, n, r)$, of the two sequences, X_i^m and Y_j^m, as the negative natural logarithm of the conditional probability $\varphi_N^{m+1}/\varphi_N^m$

$$C - FuzzyEn_{XY}(m, n, r) = -\lim_{n\to\infty} ln(\varphi_N^{m+1}/\varphi_N^m) \tag{14}$$

In fact, the number of data points N is finite, and the result obtained through the above steps is an estimate of C-FuzzyEn when the data length is N, which can be denoted as

$$C - FuzzyEn_{XY}(m, n, r, N) = ln\varphi_N^m(n, r) - ln\varphi_N^{m+1}(n, r) \tag{15}$$

For each time of C-FuzzyEn calculation, three parameters had to be determined. First is m that denotes the length of sequences or the dimension of the vector to be compared, herein, m was also set as 2. The other two parameters, i.e., r and n, determine the width and the gradient of the boundary of the exponential function, respectively. Experimentally, it is convenient to set the tolerance r between 0.1 and 0.3 and to choose small integers for the selection of n, 1 or 2. Therefore, n and r were set as 2 and 0.2, respectively.

In this study, by applying C-FuzzyEn in each 10-s-length segment, the connectivity strength between pairwise channels would be first acquired, and a 19×19 adjacency matrix would be further obtained for each segment. Thereafter, across all of these segments, for each subject, the time-varying cross-fuzzy networks that contained the inherent fuzzy fluctuation of the network architecture were formed for both Resting and LOC periods.

Apart from C-FuzzyEn, the coherence (COH) method was also adopted to construct related time-varying COH networks, to statistically compare and further validate the effectiveness of the C-FuzzyEn. As illustrated, COH can quantitatively measure the pairwise couplings in the frequency domain (i.e., the alpha band in this study) and is one of the most commonly used methods to analyze the synchrony-defined neuronal assemblies. Mathematically, COH is expressed as follows,

$$C_{XY}(f) = \frac{|S_{XY}(f)|^2}{S_{XX}(f)\, S_{YY}(f)} \tag{16}$$

where $C_{XY}(f)$ denotes the coherence coefficient of signal X_i $(1 \le i \le N)$ and Y_j $(1 \le j \le N)$, $S_{XY}(f)$ is the cross-spectrum of signal X_i $(1 \le i \le N)$ and Y_j $(1 \le j \le N)$, $S_{XX}(f)$ and $S_{YY}(f)$ are the auto-spectrum of signal X_i $(1 \le i \le N)$ and Y_j $(1 \le j \le N)$, respectively.

Similar to the C-FuzzyEn protocols, the COH strengths of pairwise nodes were first acquired at each frequency bin f per 10-s-length segment, and within the concerned alpha band ([8, 13] Hz), the corresponding 19×19 adjacency matrix was then acquired by averaging the COH values, $C_{XY}(f)$, across this specific band. And accordingly, the final COH network would be constructed for each EEG segment, which eventually formed the time-varying COH networks.

G. Network Properties

Thereafter, to further evaluate these time-varying networks during both Resting and LOC periods, two network properties, i.e., characteristic path length (CPL) and clustering coefficient (CC), would be also calculated by using the brain connectivity toolbox (BCT, http://www.nitrc.org/projects/bct/) [46]. In particular, CC indexes the functional segregation of a given

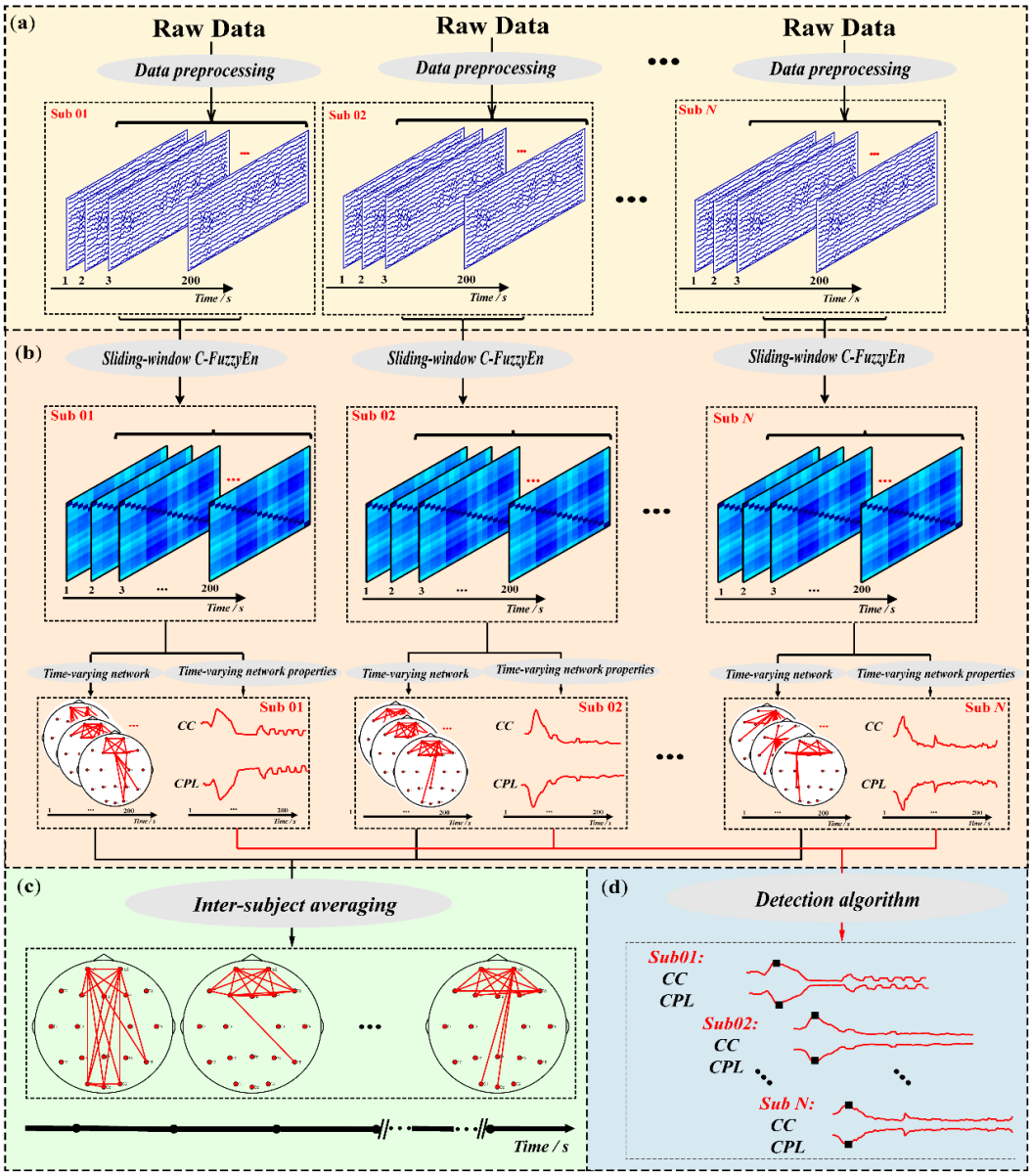

Fig. 1. Analytical protocols of the time-varying cross-fuzzy networks. (a) Raw EEG processing, (b) Time-varying cross-fuzzy networks, (c) Time-varying network architectures, and (d) Detection of patients' losing consciousness.

network and reflects the capacity for specialized processing within densely interconnected regions, while *CPL* measures the functional integration and indexes the ability to rapidly combine specialized information from distributed regions. Herein, let κ_{ij} and TN_{ij} represent the shortest weighted path length and cross fuzzy entropy coefficient ($C\text{-}FuzzyEn_{XY}$) or *COH* coefficient (C_{XY}) between network nodes i-th and j-th, respectively, Z denotes the number of nodes, and Θ denotes the set of network nodes. Then, the detailed definitions of these two properties are formulated as follows.

$$CC = \frac{1}{Z}\sum_{i\in\Theta}\frac{\sum\limits_{j,l\in\Theta}\left(TN_{ij}TN_{il}TN_{jl}\right)^{1/3}}{\sum\limits_{j\in\Theta}TN_{ij}\left(\sum\limits_{j\in\Theta}TN_{ij}-1\right)} \tag{17}$$

$$CPL = \frac{1}{Z}\sum_{i\in\Theta}\frac{\sum\limits_{j\in\Theta,j\neq i}\kappa_{ij}}{N-1} \tag{18}$$

H. Detection of Patients' Losing Their Consciousness

After the corresponding time-varying network properties within the LOC period were calculated, we also intended to testify if these parameters could be further used to detect the exact time point at which patients lost their consciousness.

Taking the injection of propofol as the starting point ('zero' point), all of these time-varying network properties then formed the time series that detailedly indexed the temporal fluctuation of the LOC. Thereafter, a related algorithm was developed to effectively capture the extreme point (i.e., the maximum point for *CC* and minimum point for *CPL*) in

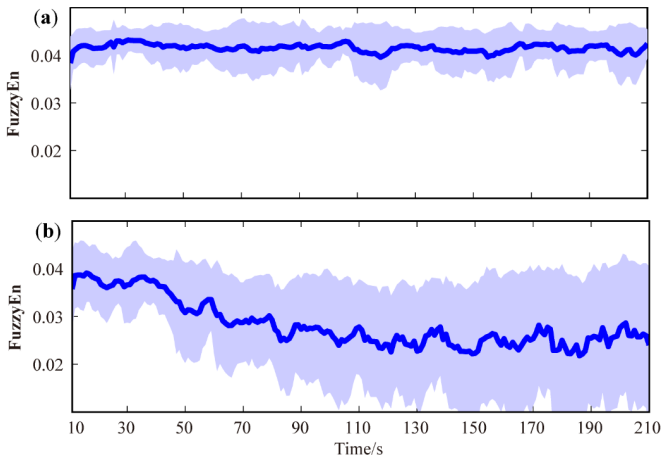

Fig. 2. The time-varying fuzzy entropy of the EEG signals corresponding to the Resting (a) and LOC (b) periods. In each subfigure, values are the means and standard deviations (Mean ± STD) of the time-varying fuzzy entropy.

the early LOC period that contained the exact time point of patients' losing their consciousness.

As reported previously, the transition from consciousness to unconsciousness induced by propofol occurred within a duration of [30, 60] s after being generally anesthetized [1], and in this study assessments from anesthesiologists clinically reported that all of these patients did lose their consciousness within this duration. Therefore, we first set a wider range of [10, 60] s, and within this defined range, the algorithm first worked to find inflection points of time-varying network properties and then acquired the maximum point of inflection points for *CC* (also the minimum point for *CPL*) of each subject, which would be defined as the time onset at which patients lost their consciousness. Herein, the details depicting how this algorithm worked were further introduced in the APPENDIX and related pseudo-codes were accordingly provided, as well.

III. Result

A. Time-Varying Fuzzy Entropy of the Single-Channel EEG Signal

Herein, within both Resting and LOC periods, we first investigated the fuzzy entropy on single-channel EEG signal by grand-averaging the fuzzy entropies across subjects per segment, which then formed the fluctuated time series of time-varying fuzzy entropies (Fig. 2). As displayed in Fig. 2, during the Resting period, the fuzzy entropy kept relatively stable; however, for the LOC, the decrease of the fuzzy entropy could be observed.

B. Time-Varying Multi-Channel Networks

Thereafter, by applying *C*-FuzzyEn and *COH* to evaluate the interactions among multiple EEG electrodes, the corresponding time-varying networks within the Resting or LOC period were first constructed for each subject and then inter-subject averaged across all subjects. Thereafter, the cost strategy with a threshold of 0.1 [47] was applied in the grand-averaged time-varying networks, and the sparse network architectures were accordingly acquired, whose scalp network topologies were then depicted in Fig. 3. Specifically investigating Fig. 3, for *C*-FuzzyEn, when looking at the topologies at rest, as displayed in Fig. 3(a), across the varied time points, a similar network architecture that coupled frontal and occipital lobes was consistently observed. On the contrary, after being generally anesthetized by using the propofol (starting at 0 s of the LOC period, Fig. 3(b)), distinctive time-varying network architectures could be observed during the early period of the LOC, as topologies fluctuated from long-range frontal-occipital to short-range prefrontal-frontal connectivity. Moreover, this fluctuation occurred around 30 s and was consistent with the anesthesiologists' clinical assessments. As for *COH*, a similar architecture underlying the time-varying networks that coupled frontal and occipital lobes was identified within the Resting period (Fig. 3(c)), as well. Unfortunately, during the late LOC period, although the corresponding network architectures were also fragmented, no specific fluctuation in network architecture could be found in Fig. 3(d). Herein, besides a cost threshold of 0.1, the time-varying networks corresponding to another cost threshold (0.05 or 0.15) also showed similar patterns as that of the threshold of 0.1, which further validated the reliability of the time-varying network architectures identified in our present study.

In the meantime, since time-varying network topologies were found to fluctuate from long-range frontal-occipital to short-range prefrontal-frontal connectivity during the LOC period, a new parameter, i.e., the long-range connectivity (LRC) that measured the number of frontal-occipital connectivity, was accordingly calculated and then investigated between the COH and C-FuzzyEn approaches. Just as displayed in Fig. 4, the distinct time-varying fluctuations of both approaches were indeed found within this period, where only C-FuzzyEn effectively captured the consciousness fluctuation induced by the GA, which was coincided with the findings depicted in Fig. 3.

Apart from the time-varying network architectures, related time-varying network properties of both periods were further investigated. Concretely, based on the fully-connected weighted time-varying matrices that had not been binarized by using any threshold, related time-varying network properties (i.e., *CC* and *CPL*) were first calculated for each subject within both Resting and LOC periods. And the formed time series of both *CC* and *CPL* were then displayed in Fig. 5. For both methods, when the brain was at rest, a similar pattern underlying the dynamics of the *CC* and *CPL*, which was coincided with that in Fig. 2(a), could be found, as a relatively stable fluctuation for either blue (i.e., *C-FuzzyEn*) or red (i.e., *COH*) solid line was displayed (Fig. 4(a)). By contrast, during the LOC period, an uphill of the *CC* and downhill of the *CPL* could only be found in the blue solid line (i.e., *C-FuzzyEn*, Fig. 5(b)), which was around a time range of [20, 40] s. While the dynamics of the time-varying network properties derived from the *COH* showed indistinctive fluctuations and insignificant changes in the red solid line (Fig. 5(b)) could be found during the whole LOC period. Moreover, for both methods, the corresponding time-varying network properties were first averaged across either Resting or LOC period, and

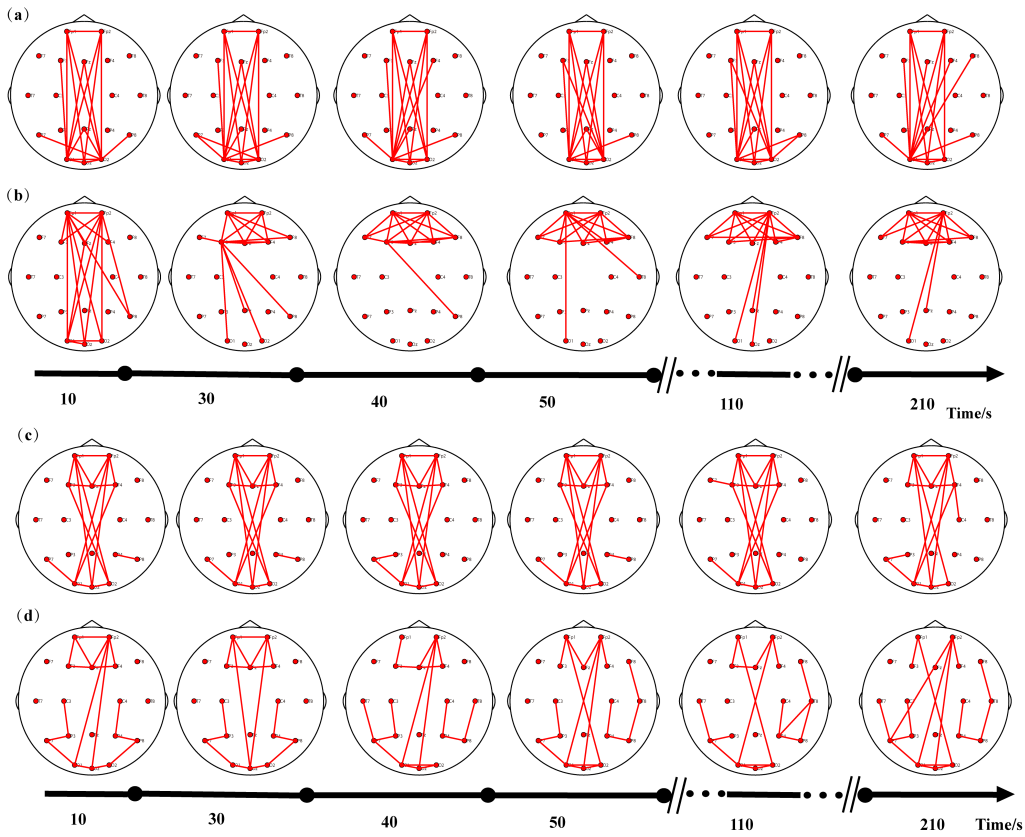

Fig. 3. The time-varying network architecture estimated by the C-FuzzyEn and COH methods. (a) Resting period of C-FuzzyEn, (b) LOC of C-FuzzyEn, (c) Resting period of COH, and (d) LOC of COH.

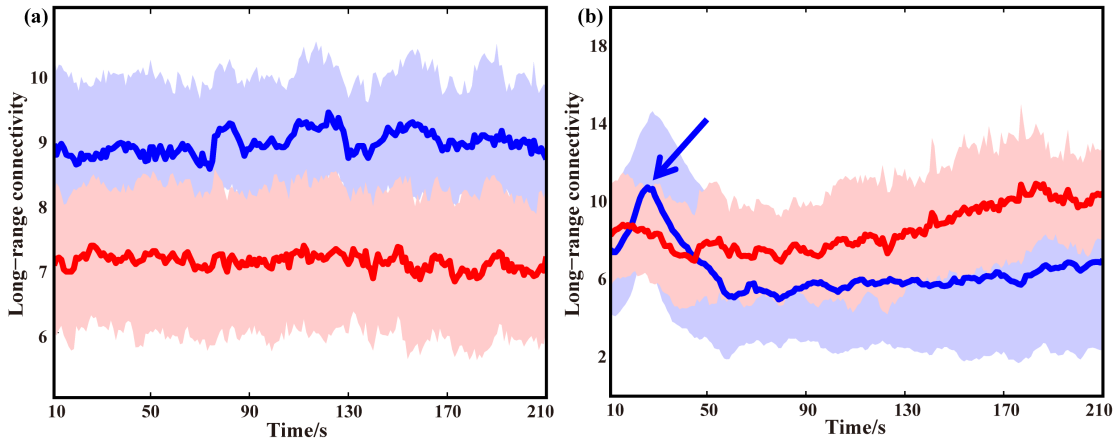

Fig. 4. The time-varying LRC parameter corresponding to the C-FuzzyEn and COH approaches during the Resting (a) and LOC (b) period. The red and blue solid lines denote the mean number of the long-range frontal-occipital connectivity of COH and C-FuzzyEn, respectively, the pink and light blue shadows denote the corresponding standard deviation of COH and C-FuzzyEn, respectively.

these averaged network properties were further statistically compared between both periods by applying the paired t-test. Herein, the *CPL* of the LOC period was consistently identified to be significantly larger ($p < 0.05$) than that of the Resting period, while the *CC* of the LOC period was relatively smaller than that of the Resting period.

As the temporal fluctuation in the time-varying *C*-FuzzyEn network properties was identified within the LOC period (Fig. 5(b)), an algorithm was then developed to quantitatively detect the time onset (in seconds) of patients' losing their consciousness induced by propofol. As listed in Table I, the varied temporal durations were quantitatively identified, when the *CC* and *CPL* reached their zenith and nadir, respectively, that was, our developed algorithm found around 31.5 $\pm$ 8.6 s, patients would lose their consciousness.

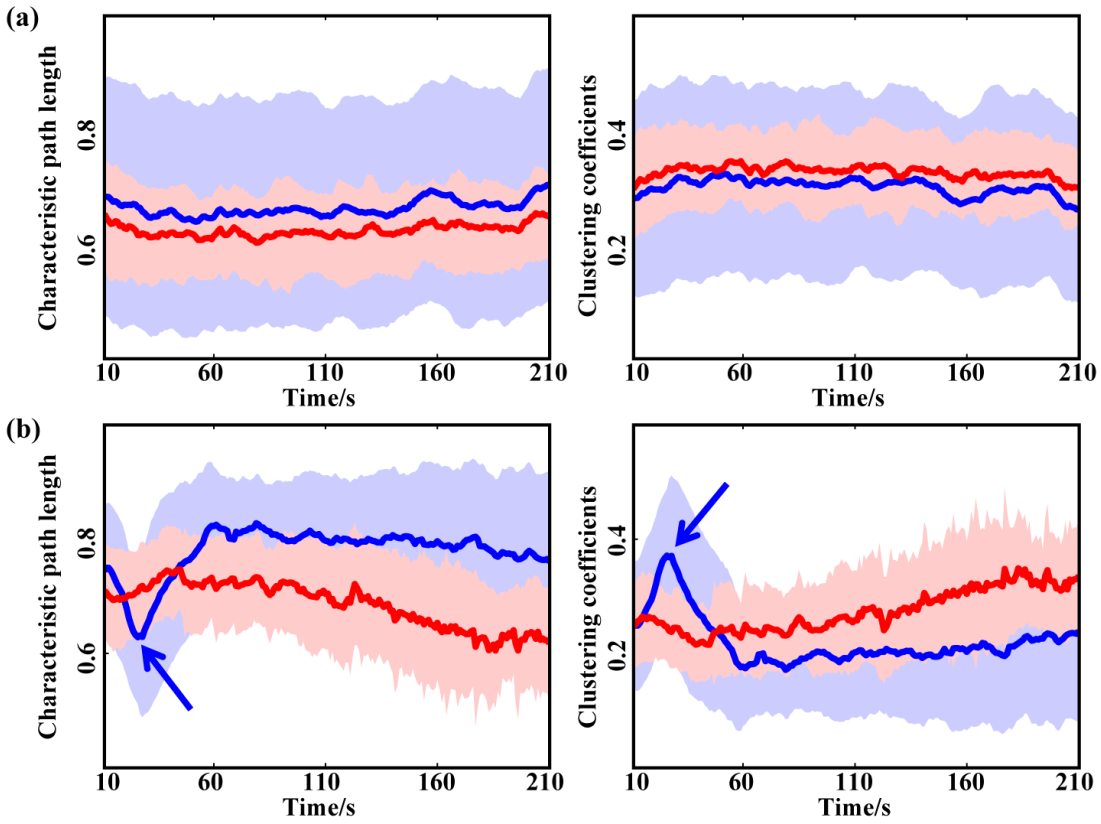

Fig. 5. The time-varying C-FuzzyEn and COH network properties for both Resting (a) and LOC (b) period. The blue and red solid lines illustrate the fluctuation of the C-FuzzyEn and COH network properties, respectively. In each subfigure, values are the means and standard deviations (Mean ± STD) of the properties of the time-varying networks.

TABLE I
THE TIME ONSET AT WHICH PATIENTS LOST THEIR CONSCIOUSNESS DETECTED BY OUR DEVELOPED ALGORITHM

Subject	Time Onset (s)	Subject	Time Onset (s)	Subject	Time Onset (s)
Sub01	23	Sub12	36	Sub23	29
Sub02	24	Sub13	25	Sub24	28
Sub03	42	Sub14	29	Sub25	31
Sub04	46	Sub15	26	Sub26	38
Sub05	18	Sub16	22	Sub27	26
Sub06	36	Sub17	29	Sub28	35
Sub07	34	Sub18	51	Sub29	28
Sub08	23	Sub19	30	Sub30	23
Sub09	53	Sub20	28	**Mean ± STD**	31.5 ± 8.6
Sub10	31	Sub21	44		
Sub11	33	Sub22	25		

IV. DISCUSSION

The human brain functions as a large-scale network that is the neural basis of the efficient transition and processing of the perceived information. GA is usually interpreted as a network disruption, and the dysfunctions of certain regions induced by GA, especially the long-range frontal-occipital disconnectivity, disturb the information processing in the brain and lead to network dysfunction [48], as well as unconsciousness [49]. In this study, to achieve accurate consciousness detection, based on the single-channel EEG series, the corresponding fuzzy entropy was first assessed. Thereafter, by applying the *C*-FuzzyEn in multi-channel EEG datasets, we further developed an approach to construct the time-varying *C*-FuzzyEn networks within both periods and finally put forward an algorithm to quantitatively detect the time point at which patients lost their consciousness.

As displayed in Fig. 2, the time-varying fuzzy fluctuation on single-channel series was first obtained by grand-averaging the fuzzy entropies across patients, which provided the opportunity to primarily investigate the time-varying dynamics of the brain activity during both Resting and LOC periods. As reported in previous studies, during the resting state, the brain usually stays under a relatively stable level [50], [51],

the corresponding brain configuration guarantees the stable consciousness state, when applying related index (e.g., fuzzy entropy) to evaluate the corresponding activity during this period, across the whole time scales, the stable time-varying fuzzy entropy could thus be acquired, as displayed in Fig. 2(a). On the contrary, after being generally anesthetized by injecting propofol, as expected, the stable inner state in the patient's brain was broken subsequently, and the fuzzy level maintained in the brain was then disrupted and then fluctuated across the LOC period. Herein, specifically investigating Fig. 2(b), the corresponding time-varying fuzzy entropy did validate the disrupted complexity of related brain activity across the LOC period, as the decrease in time-varying fuzzy entropy could be found from Fig. 2(b).

In fact, numerous studies have consistently demonstrated a breakdown of the brain network during unconsciousness [25], investigating the single-channel fuzzy characteristics could only identify the potential dysfunction that occurs during both periods but was helpless for monitoring the LOC clinically and also left the network fluctuation being unveiled. Therefore, in this study, we then expanded our investigations from single- to multi-channel EEG analyses, by developing a related approach to construct the time-varying cross-fuzzy networks. And we explored if the network disconnectivity occurred during both periods, as well as how the brain networks fluctuating, whose results were further validated by the traditional *COH* method.

When comparing the acquired time-varying networks and related network properties of both methods, as displayed in Figs. 3, 4, and 5, during the Resting period, both methods could consistently capture the inherent brain activity, as the relatively stable long-range frontal-occipital connectivity was identified and then quantitatively measured by the LRC parameter (Fig. 4(a)). However, after being anesthetized by propofol, the stabilization of homeostasis in the brain was disrupted, and related brain networks then fluctuated during the LOC period accordingly. When specifically exploring the corresponding results during the LOC period, unfortunately, for the *COH*, only the disrupted frontal-occipital connectivity was identified across the whole time scales, as well as the decreased network properties (Fig. 5(b)), no fluctuated network patterns could be found (Fig. 3(d)). On the contrary, the *C-FuzzyEn* not only captured the disrupted network connectivity but also identified the fluctuated network pattern, as displayed in Figs. 3(b) and 5(b), the inherent pattern transited from long-range frontal-occipital to inner-frontal connectivity, as well as the fluctuated network properties, which was consistent with previous studies [50], [52], [53]. In the meantime, the corresponding LRC parameter further indicated that only C-FuzzyEn effectively captured the disrupted long-range frontal-occipital connectivity induced by the GA (Fig. 4(b)). As illustrated, since the EEG is non-linear and non-stationary, when the fluctuation in brain networks occurred, traditional methods, such as *COH*, fail in capturing related fluctuations in brain activity; on the contrary, *C-FuzzyEn* expertizes in quantitatively uncover the dynamic fluctuations in related brain networks, which thus not only deepen our understanding of consciousness fluctuation during the GA but also helps monitor the LOC. Therefore, based on the *C-FuzzyEn*, the time-varying networks and related network properties were further explored to first uncover the mechanism of LOC and then develop a proper algorithm to detect the exact time at which patients lost their consciousness.

As displayed in Fig 3(a), when tracking the dynamic transition of the time-varying networks at rest, since no external information was perceived and integrated, the long-range frontal-occipital connectivity was maintained stable during the whole period, which was coincided with that identified in Fig. 2(a) and related previous studies [54], [55]. By contrast, loss of consciousness during general anesthesia has been illustrated to be caused by a breakdown of the network connectivity [48]. As demonstrated, GA focuses on the frontal lobe, especially the functional connectivity that couples the anterior and posterior brain areas [22], [56]. During the GA, the default mode network flow was broken [25], [52], [53], which was consistent with the findings in our present study. Herein, we did find the long-range connectivity coupling frontal and occipital lobes were disrupted during GA (Fig. 3(b)), especially around a range of [20, 40] s after being propofol-induced [57], [58], while in the later LOC stage, the network fragmentation coupling the frontal area was identified [25]. GA does not seem to grossly impair all linked networks [48]–[50], when the depth of anesthesia is characterized by the subject's unresponsiveness, a partial rather than complete reduction in connectivity could be generally observed [24]. Therefore, in our present study, although the long-range connectivity was disrupted in the early stage, the inner frontal linkages increased in the later LOC stage, which was coincided with Vlisides's findings [27].

Moreover, when specifically investigating the time-varying network properties (*CC* and *CPL*) during both periods in Fig. 5, the relatively stable fluctuation of the network properties at rest was first unveiled, and this was similar to that displayed in both Figs. 2(a) and 3(a). However, in the early propofol-induced LOC stage, the uphill of the *CC* and downhill of the *CPL* around a range of [20, 40] s could be found (blue solid line in Fig. 5(b)), along with patients' losing their consciousness, thereafter, corresponding parameters decreased. We suspected that the time points underlying the highest *CC* and the lowest *CPL* might be the point at which patients lost their consciousness, and this was indeed consistent with the clinical assessments reported by the anesthesiologists. As illustrated, after the propofol was injected, the patients' brain started to fluctuate excessively [59], [60], which was effectively captured by the *CC* and *CPL* calculated, as the increased *CC* and decreased *CPL* could be found from Fig. 5(b) in the early LOC period. However, after being deeply anesthetized (the later stage of LOC), the brain activity will be inhibited due to the effect of anesthetic drugs, and related information exchange would be then reduced [58], [61], therefore, the time-varying network properties decreased to a relatively low level during the later LOC stage.

Since this fluctuated pattern was identified in our present study, if this could be further used for consciousness monitoring clinically? Herein, as suggested, based on the time-varying *C-FuzzyEn* network properties, a possible algorithm

was further developed to detect the time onset at which patients lost their consciousness, within the duration of [10, 60] s after being injected with propofol. As depicted, the assessments from anesthesiologists clinically reported that all of these patients lost their consciousness around a range of [20, 40] s after being anesthetized; for each patient, as listed in Table I, our developed algorithm did identify that around 31.5 ± 8.6 s, the related extreme point was detected and marked as the time point (in seconds) of patients' losing consciousness, which further validated the capacity of our developed algorithm for monitoring consciousness clinically.

V. Conclusion

In conclusion, by applying multi-channel EEG analysis, the corresponding time-varying cross-fuzzy networks were constructed, and we then explored the potential differences in cross-fuzzy network fluctuations during the Resting and LOC periods. In detail, when the brain was rest, the relatively stable fuzzy fluctuations corresponding to the time series, dynamic networks, and network properties were found. However, during the LOC period, the long-range connectivity coupling frontal and occipital lobes were disrupted, and specifically investigating the early LOC stage, the uphill of the *CC* and downhill of the *CPL* under anesthesia were further identified around a range of [20, 40] s after being anesthetized, and related detection algorithm was finally put forward, which did effectively capture the time point at which patients lost their consciousness. These findings might be the key to explain and also identify the loss of consciousness clinically, which would also provide a potential tool for accurately monitoring patients' anesthetic consciousness state.

Appendix

Herein, based on the calculated time-varying *C-FuzzyEn* network properties, the detection algorithm for monitoring patients' anesthetic consciousness state clinically was further developed in compliance with following steps.

Step 1. Calculating the 19×19 *C-FuzzyEn* matrix at each time point for each patient;

Step 2. Calculating the time-varying *C-FuzzyEn* network properties (*CPL* and *CC*) for each time point, and the *CPL* and *CC* values at each time point then formed the temporal series of the time-varying *CPL* and *CC* for each patient;

Step 3. Calculating inflection points of the time-varying *CPL* and *CC* with a time range of [10, 60] s for each patient;

Step 4. Calculating the maximum point of inflection points for *CC* (also the minimum point of inflection points for *CPL*) for each patient.

Step 5. Defining the time point at which patients lost their consciousness by using the maximum point of inflection points for *CC* (also the minimum point of inflection points for *CPL*).

Moreover, to guarantee our developed algorithm to be clear and easy-understanding, the corresponding pseudo-codes were further depicted below.

Step 1. Calculating *C-FuzzyEn* matrix C for each patient;

Step 2. For $i = 1$ to M, (M represents the whole patient)
For $j = 1$ to N, (N represents the whole time point)
CPL (i, j) = BCT for CPL ($C(:, :, j, i)$ for each patient j at time point i);
CC (i, j) = BCT for $CC(C(:, :, j, i)$ for each patient j at time point i);
EndFor
EndFor

Step 3. For $i = 1$ to M
Inflection points $CPLI$ = findpeaks (CPL (i, 10:60));
Inflection points CCI = findpeaks (CC (i, 10:60));
EndFor

$CPLT$ = min ($CPLI$);
CCT = max (CCI).

References

[1] E. N. Brown, R. Lydic, and N. D. Schiff, "General anesthesia, sleep, and coma," *New England J. Med.*, vol. 363, no. 27, pp. 2638–2650, Dec. 2010.

[2] P. L. Purdon *et al.*, "Electroencephalogram signatures of loss and recovery of consciousness from propofol," *Proc. Nat. Acad. Sci. USA*, vol. 110, no. 12, pp. E1142–E1151, Mar. 2013.

[3] M. S. Avidan *et al.*, "Prevention of intraoperative awareness in a high-risk surgical population," *New England J. Med.*, vol. 365, no. 7, pp. 591–600, Aug. 2011.

[4] K. Leslie and M. P. Chan, "Posttraumatic stress disorder in aware patients from the B-aware trial," *Anesthesia Analgesia*, vol. 110, no. 3, pp. 823–828, 2010.

[5] G. Wang *et al.*, "Monitoring the depth of anesthesia through the use of cerebral hemodynamic measurements based on sample entropy algorithm," *IEEE Trans. Biomed. Eng.*, vol. 67, no. 3, pp. 807–816, Mar. 2020.

[6] D. A. Chernik *et al.*, "Validity and reliability of the observer's assessment of alertness/sedation scale: Study with intravenous midazolam," *J. Clin. Psychopharmacol.*, vol. 10, no. 4, pp. 244–251, Aug. 1990.

[7] P. S. Glass, M. Bloom, L. Kearse, C. Rosow, P. Sebel, and P. Manberg, "Bispectral analysis measures sedation and memory effects of propofol, midazolam, isoflurane, and alfentanil in healthy volunteers," *Anesthesiology*, vol. 86, no. 4, pp. 836–847, Apr. 1997.

[8] A. Ranft *et al.*, "Neural correlates of sevoflurane-induced unconsciousness identified by simultaneous functional magnetic resonance imaging and electroencephalography," *Anesthesiology*, vol. 125, no. 5, pp. 861–872, Nov. 2016.

[9] P. E. Vlisides *et al.*, "Neurophysiologic correlates of ketamine sedation and anesthesia: A high-density electroencephalography study in healthy volunteers," *Anesthesiology*, vol. 127, no. 1, pp. 58–69, Jul. 2017.

[10] S. N. Ching, A. Cimenser, P. L. Purdon, E. N. Brown, and N. J. Kopell, "Thalamocortical model for a propofol-induced α-rhythm associated with loss of consciousness," *Proc. Nat. Acad. Sci. USA*, vol. 107, no. 52, pp. 22665–22670, Dec. 28 2010.

[11] P. L. Purdon, A. Sampson, K. J. Pavone, and E. N. Brown, "Clinical electroencephalography for anesthesiologists: Part I: Background and basic signatures," *Anesthesiology*, vol. 123, no. 4, pp. 937–960, Oct. 2015.

[12] K. Bauerle, "Prediction of depth of sedation and anaesthesia by the Narcotrend EEG monitor," *Brit. J. Anaesthesia*, vol. 92, no. 6, p. 912, Jun. 2004.

[13] R. Ní Mhuircheartaigh, C. Warnaby, R. Rogers, S. Jbabdi, and I. Tracey, "Slow-wave activity saturation and thalamocortical isolation during propofol anesthesia in humans," *Sci. Transl. Med.*, vol. 5, p. 208, Oct. 2013.

[14] R. K. Ellerkmann *et al.*, "The entropy module and bispectral index as guidance for propofol-remifentanil anaesthesia in combination with regional anaesthesia compared with a standard clinical practice group," *Anaesthesia Intensive Care*, vol. 38, no. 1, pp. 159–166, Jan. 2010.

[15] J. Bruhn, P. S. Myles, R. Sneyd, and M. M. R. F. Struys, "Depth of anaesthesia monitoring: What's available, what's validated and what's next?" *Brit. J. Anaesthesia*, vol. 97, no. 1, pp. 85–94, Jun. 2006.

[16] Y. Wang, Z. Liang, L. J. Voss, J. W. Sleigh, and X. Li, "Multi-scale sample entropy of electroencephalography during sevoflurane anesthesia," *J. Clin. Monitor. Comput.*, vol. 28, no. 4, pp. 409–417, Aug. 2014.

[17] Z. Cao and C.-T. Lin, "Inherent fuzzy entropy for the improvement of EEG complexity evaluation," *IEEE Trans. Fuzzy Syst.*, vol. 26, no. 2, pp. 1032–1035, Apr. 2018.

[18] Z. Cao *et al.*, "Extraction of SSVEPs-based inherent fuzzy entropy using a wearable headband EEG in migraine patients," *IEEE Trans. Fuzzy Syst.*, vol. 28, no. 1, pp. 14–27, Jan. 2020.

[19] R. Zhang, F. Li, T. Zhang, D. Yao, and P. Xu, "Subject inefficiency phenomenon of motor imagery brain-computer interface: Influence factors and potential solutions," *Brain Sci. Adv.*, vol. 6, no. 3, pp. 224–241, Sep. 2020.

[20] P. Li *et al.*, "EEG based emotion recognition by combining functional connectivity network and local activations," *IEEE Trans. Biomed. Eng.*, vol. 66, no. 10, pp. 2869–2881, Oct. 2019.

[21] F. Li *et al.*, "Differentiation of schizophrenia by combining the spatial EEG brain network patterns of rest and task P300," *IEEE Trans. Neural Syst. Rehabil. Eng.*, vol. 27, no. 4, pp. 594–602, Apr. 2019.

[22] S. Dehaene and J. P. Changeux, "Experimental and theoretical approaches to conscious processing," *Neuron*, vol. 70, no. 2, pp. 200–227, Apr. 2011.

[23] J. R. King *et al.*, "Information sharing in the brain indexes consciousness in noncommunicative patients," *Current Biol.*, vol. 23, no. 19, pp. 1914–1919, Oct. 2013.

[24] F. Ferrarelli *et al.*, "Breakdown in cortical effective connectivity during midazolam-induced loss of consciousness," *Proc. Nat. Acad. Sci. USA*, vol. 107, no. 6, pp. 2681–2686, Feb. 2010.

[25] G. A. Mashour and A. G. Hudetz, "Neural correlates of unconsciousness in large-scale brain networks," *Trends Neurosci.*, vol. 41, no. 3, pp. 150–160, Mar. 2018.

[26] A. E. Hudson, "Metastability of neuronal dynamics during general anesthesia: Time for a change in our assumptions?" *Frontiers Neural Circuits*, vol. 11, p. 58, Aug. 2017.

[27] P. E. Vlisides *et al.*, "Dynamic cortical connectivity during general anesthesia in surgical patients," *Anesthesiology*, vol. 130, no. 6, pp. 885–897, Jun. 2019.

[28] O. Bodart *et al.*, "Global structural integrity and effective connectivity in patients with disorders of consciousness," *Brain Stimulation*, vol. 11, no. 2, pp. 358–365, Mar. 2018.

[29] U. Lee, S. Ku, G. Noh, S. Baek, B. Choi, and G. A. Mashour, "Disruption of frontal–parietal communication by ketamine, propofol, and sevoflurane," *Anesthesiology*, vol. 118, no. 6, pp. 1264–1275, Jun. 2013.

[30] D. Li and G. A. Mashour, "Cortical dynamics during psychedelic and anesthetized states induced by ketamine," *NeuroImage*, vol. 196, pp. 32–40, Aug. 2019.

[31] S. Sarasso *et al.*, "Consciousness and complexity during unresponsiveness induced by propofol, xenon, and ketamine," *Current Biol.*, vol. 25, no. 23, pp. 3099–3105, Dec 7 2015.

[32] C. J. Stam and B. W. van Dijk, "Synchronization likelihood: An unbiased measure of generalized synchronization in multivariate data sets," *Phys. D, Nonlinear Phenomena*, vol. 163, nos. 3–4, pp. 236–251, 2002.

[33] Z. Liang *et al.*, "EEG entropy measures in anesthesia," *Frontiers Comput. Neurosci.*, vol. 9, p. 16, Feb. 2015.

[34] H.-B. Xie, J.-Y. Guo, and Y.-P. Zheng, "A comparative study of pattern synchronization detection between neural signals using different cross-entropy measures," *Biol. Cybern.*, vol. 102, no. 2, pp. 123–135, Feb. 2010.

[35] H.-B. Xie, Y.-P. Zheng, J.-Y. Guo, and X. Chen, "Cross-fuzzy entropy: A new method to test pattern synchrony of bivariate time series," *Inf. Sci.*, vol. 180, no. 9, pp. 1715–1724, 2010.

[36] P. Li, C. Liu, X. Wang, B. Li, W. Che, and C. Liu, "Cross-sample entropy and cross-fuzzy entropy for testing pattern synchrony: How results vary with different threshold value *r*," in *Proc. World Congr. Med. Phys. Biomed. Eng.*, Beijing, China, May 2013, pp. 485–488.

[37] P. Xu *et al.*, "Differentiating between psychogenic nonepileptic seizures and epilepsy based on common spatial pattern of weighted EEG resting networks," *IEEE Trans. Biomed. Eng.*, vol. 61, no. 6, pp. 1747–1755, Jun. 2014.

[38] M. Murias, J. M. Swanson, and R. Srinivasan, "Functional connectivity of frontal cortex in healthy and ADHD children reflected in EEG coherence," *Cerebral Cortex*, vol. 17, no. 8, pp. 1788–1799, Aug. 2007.

[39] L. Dong *et al.*, "MATLAB toolboxes for reference electrode standardization technique (REST) of scalp EEG," *Frontiers Neurosci.*, vol. 11, p. 601, Oct. 2017.

[40] D. Yao, "A method to standardize a reference of scalp EEG recordings to a point at infinity," *Physiol. Meas.*, vol. 22, no. 4, p. 693, 2001.

[41] A. Cimenser *et al.*, "Tracking brain states under general anesthesia by using global coherence analysis," *Proc. Nat. Acad. Sci. USA*, vol. 108, no. 21, pp. 8832–8837, May 2011.

[42] U. R. Acharya, H. Fujita, V. K. Sudarshan, S. Bhat, and J. E. Koh, "Application of entropies for automated diagnosis of epilepsy using EEG signals: A review," *Knowl. Based Syst.*, vol. 88, pp. 85–96, Nov. 2015.

[43] W. Chen, J. Zhuang, W. Yu, and Z. Wang, "Measuring complexity using FuzzyEN, ApEn, and SampEN," *Med. Eng. Phys.*, vol. 31, no. 1, pp. 61–68, Jan. 2009.

[44] S. M. Pincus, "Approximate entropy as a measure of system complexity," *Proc. Nat. Acad. Sci. USA*, vol. 88, no. 6, pp. 2297–2301, Mar. 1991.

[45] W. Chen, Z. Wang, H. Xie, and W. Yu, "Characterization of surface EMG signal based on fuzzy entropy," *IEEE Trans. Neural Syst. Rehabil. Eng.*, vol. 15, no. 2, pp. 266–272, Jun. 2007.

[46] M. Rubinov and O. Sporns, "Complex network measures of brain connectivity: Uses and interpretations," *NeuroImage*, vol. 52, no. 3, pp. 1059–1069, 2010.

[47] F. Li *et al.*, "The dynamic brain networks of motor imagery: Time-varying causality analysis of scalp EEG," *Int. J. Neural Syst.*, vol. 29, no. 1, Feb. 2019, Art. no. 1850016.

[48] M. Boly *et al.*, "Connectivity changes underlying spectral EEG changes during propofol-induced loss of consciousness," *J. Neurosci.*, vol. 32, no. 20, pp. 7082–7090, May 2012.

[49] L. Naci *et al.*, "Functional diversity of brain networks supports consciousness and verbal intelligence," *Sci. Rep.*, vol. 8, no. 1, p. 13259, Sep. 2018.

[50] F. Li *et al.*, "Inter-subject P300 variability relates to the efficiency of brain networks reconfigured from resting- to task-state: Evidence from a simultaneous event-related EEG-fMRI study," *NeuroImage*, vol. 205, Jan. 2020, Art. no. 116285.

[51] H. H. Shen, "Core concept: Resting-state connectivity," *Proc. Nat. Acad. Sci. USA*, vol. 112, no. 46, pp. 14115–14116, Nov. 2015.

[52] J. A. Hashmi *et al.*, "Dexmedetomidine disrupts the local and global efficiencies of large-scale brain networks," *Anesthesiology*, vol. 126, no. 3, pp. 419–430, Mar. 2017.

[53] A. G. Hudetz, "General anesthesia and human brain connectivity," *Brain Connectivity*, vol. 2, no. 6, pp. 291–302, Dec. 2012.

[54] F. Li *et al.*, "Relationships between the resting-state network and the P3: Evidence from a scalp EEG study," *Sci. Rep.*, vol. 5, p. 15129, Feb. 2015.

[55] F. Li *et al.*, "Reconfiguration of brain network between resting state and P300 task," *IEEE Trans. Cognit. Develop. Syst.*, vol. 13, no. 2, pp. 383–390, Jun. 2021.

[56] J. P. Changeux, "Conscious processing: Implications for general anesthesia," *Current Opinion Anesthesiol.*, vol. 25, no. 4, pp. 397–404, Aug. 2012.

[57] M. S. Schroter *et al.*, "Spatiotemporal reconfiguration of large-scale brain functional networks during propofol-induced loss of consciousness," *J. Neurosci.*, vol. 32, no. 37, pp. 12832–12840, Sep. 2012.

[58] J. Schrouff, "Brain functional integration decreases during propofol-induced loss of consciousness," *NeuroImage*, vol. 57, no. 1, pp. 198–205, 2011.

[59] L. D. Lewis *et al.*, "Rapid fragmentation of neuronal networks at the onset of propofol-induced unconsciousness," *Proc. Nat. Acad. Sci. USA*, vol. 109, no. 49, pp. E3377–E3386, Dec. 2012.

[60] G. A. Mashour, "Consciousness, anesthesia, and neural synchrony," *Anesthesiology*, vol. 119, no. 1, pp. 7–9, Jul. 2013.

[61] U. Lee, G. A. Mashour, S. Kim, G.-J. Noh, and B.-M. Choi, "Propofol induction reduces the capacity for neural information integration: Implications for the mechanism of consciousness and general anesthesia," *Consciousness Cognition*, vol. 18, no. 1, pp. 56–64, Mar. 2009.